1 Theory of Elementary Particles

M. Bordone, S. Borowka, F. Cascioli, J. Currie, T. Gehrmann, M. Grazzini, A. Greljo, A. Ilnicka, G. Isidori, M. Jaquier, S. Kallweit, D. Kara, J. Lindert, A. Lo Presti, P. Lowdon, P. Maierhöfer, D. Marzocca, N. Moretti, J. Niehues, G. Oeztürk, A. Papaefstathiou, M. Patra, A. Pattori, S. Pozzorini, D. Rathlev, H. Sargsyan, M. Schönherr, A. Signer, L. Tancredi, A. Torre, P. Torrielli, A. Visconti, E. Weihs, M. Wiesemann, D. Wyler

in collaboration with: Durham University, INFN Firenze, University of Buenos Aires, Freiburg University, Mainz University, INFN Milano, MPI Munich, INFN Padova, Peking University, Oxford University, INFN Roma, SLAC, ETH Zürich, Desy Hamburg, TU Dresden

The particle theory group at the Physik-Institut is primarily involved in research projects dealing with the interpretation of data from high energy particle colliders. Topics are precision calculations of benchmark observables, simulation of full collider events, identification of optimal observables for searches and measurements, physics beyond the Standard Model, as well as development of calculational techniques.

We summarize some highlights of last year's research below.

1.1 Vector boson pair production at NNLO

The Tevatron experiments have measured cross sections for vector-boson pair production at invariant masses beyond those probed at LEP2, setting limits on anomalous couplings, and this program is continued at the LHC [1].

The study of the production of vector-boson pairs (VV') is relevant for physics both within and beyond the Standard Model (SM). First of all, any deviation of the vector boson trilinear couplings from the structure predicted by $SU(2) \otimes U(1)$ gauge invariance would be a signal of new physics. At the same time vector boson pairs provide a dominant background in new physics searches. Although the Higgs resonance was observed well below the WW and ZZ thresholds, off-shell WW and ZZ backgrounds must be taken into account when extracting the Higgs signal and width.

Until just one year ago, theoretical predictions for VV' production were essentially limited to next-to-leading order (NLO) in perturbative QCD. The bottleneck has been the knowledge of the relevant two-loop amplitudes. At next-to-next-to-leading order (NNLO) tree-level scattering amplitudes with two additional (unresolved) partons, one-loop amplitudes with one additional parton, and one-loop-squared and two-loop corrections to the Born subprocess $q\bar{q} \to VV'$ must be evaluated.

Recently, a major step forward was made with the evaluation of all two-loop planar [2, 3] and non-planar [4, 5] master integrals relevant for the production of off-shell vector boson pairs, and the calculation of the corresponding helicity amplitudes has been completed [6]. Still, the computation of the NNLO corrections is non-trivial. Infrared (IR) singularities at intermediate stages of the calculation forbid straightforward numerical techniques. To handle and cancel these singularities the q_T subtraction formalism [7] is well suited since it is fully developed to work in the hadronic production of heavy colorless final states.

In the following we present results for ZZ [8] and WW [9] production in pp collisions with $\sqrt{s}$ ranging from 7 to 14 TeV. The required tree-level and one-loop amplitudes were obtained with the OpenLoops [10] generator, which employs the Denner-Dittmaier algorithm for the numerical evaluation of one-loop integrals and implements a fast numerical recursion for the calculation of NLO scattering amplitudes within the SM.

As for the EW couplings, we use the so-called G_μ scheme, with $G_F = 1.16639 \times 10^{-5}$ GeV^{-2}, $m_W = 80.399$ GeV and $m_Z = 91.1876$ GeV. Additional input, $m_t = 173.2$ GeV and $m_H = 125$ GeV, enters through the loop-induced gluon fusion contribution. We use the MSTW 2008 [11] sets of parton distributions, with densities and α_S evaluated at each corresponding order (i.e., we use $(n+1)$-loop α_S at N^{n}LO, with $n = 0, 1, 2$), and we consider $N_f = 5$ massless quark flavors. The default renormalization (μ_R) and factorization (μ_F) scales are set to $\mu_R = \mu_F = m_Z$.

1.1.1 *ZZ*

The resulting LO, NLO and NNLO ZZ cross sections as a function of $\sqrt{s}$ are shown in Fig. 1.1. For comparison, we also show the NLO result supplemented with the loop-induced gluon fusion contribution ("NLO+gg") computed with NNLO parton distribution functions (PDFs). The NLO corrections increase the LO result by about 45%. The impact of NNLO corrections with respect to the NLO result ranges from 11% ($\sqrt{s} = 7$ TeV) to 17% ($\sqrt{s} = 14$ TeV), see lower panel in Fig. 1.1. Using NNLO PDFs throughout, the gluon fusion contribution exhausts between 58% and 62% of the full NNLO correction. The theoretical predictions are compared with the ATLAS and CMS values measured at $\sqrt{s} = 7$ TeV and $\sqrt{s} = 8$ TeV. The experimental results still have relatively large uncertainties and are compatible with both the NLO and NNLO predictions with the possible exception of the ATLAS measurement at $\sqrt{s} = 8$ TeV which seems to prefer a lower cross section. Such comparisons should be interpreted with care since the LHC experiments base their ZZ production cross section on four-lepton final states with dilepton invariant mass around the Z boson mass: the contribution from far off-shell Z bosons is excluded. Furthermore, EW corrections are not included in our calculation and are expected to lower the inclusive cross section.

In Table 1.1 we list the LO, NLO and NNLO cross sections and scale uncertainties, evaluated by varying μ_R and μ_F simultaneously and independently in the range $0.5m_Z{<}\mu_R, \mu_F{<}2m_Z$ with the constraint $0.5{<}\mu_F/\mu_R{<}2$. Scale uncertainties are $O(\pm 3\%)$ for both NLO and NNLO. Note that the NLO scale uncertainty does not cover the NNLO effect which is no surprise since the gluon fusion channel, which provides a rather large contribution, opens up at NNLO only.

1.1.2 *WW*

Contrary to what happens in ZZ production, the higher-order QCD corrections to WW production include partonic channels with b-quarks in the final state, which leads to a subtle interplay between WW and top production. In the five-flavor-number scheme (5FNS), where b-quarks are included in the parton distribution functions with their mass set to zero, the presence of real b-quark emission is crucial in order to cancel collinear singularities that arise from $g \to b\bar{b}$ splittings in the virtual corrections. At the same time, the occurrence of Wb pairs in the real-emission matrix elements induces top-quark resonances that lead to a problematic contamination of WW production. This problem can be circumvented in the four-flavor scheme (4FNS) where, since b-quarks are massive and collinear divergences are not present, we can define top-free WW production by simply omitting b-quark emissions.

We present LO, NLO and NNLO predictions for $pp \to W^+W^-X$ in the 4FNS with $\sqrt{s}$ ranging from 7 to 14 TeV. We use the MSTW2008 sets of PDFs with four active flavors. The default renormalization (μ_R) and factorization

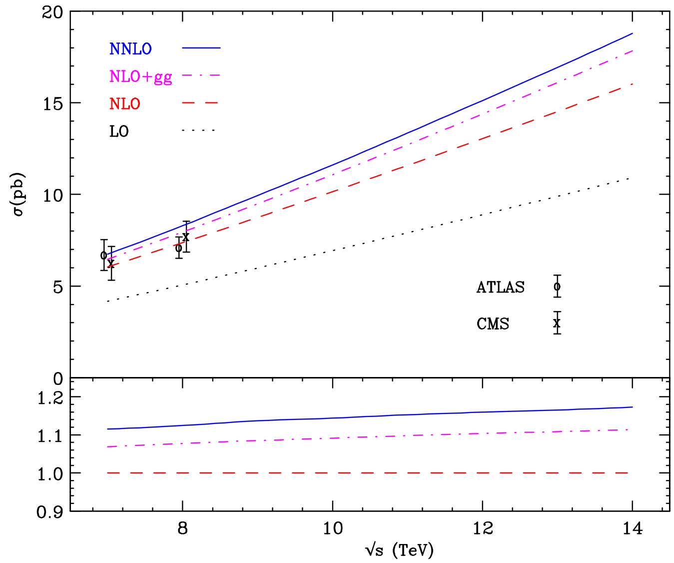

FIG. 1.1 –
Top: ZZ cross section at LO, NLO, NLO+gg and NNLO as a function of $\sqrt{s}$. The ATLAS and CMS results at $\sqrt{s} = 7$ TeV and $\sqrt{s} = 8$ TeV are shown for comparison.
Bottom: NNLO and NLO+gg results normalized to the NLO prediction.

TAB. 1.1 –
Inclusive cross section for ZZ production at the LHC at LO, NLO and NNLO with $\mu_F = \mu_R = m_Z$. The uncertainties are obtained by varying the renormalization and factorization scales in the range $0.5m_Z < \mu_R, \mu_F < 2m_Z$ with the constraint $0.5 < \mu_F/\mu_R < 2$.

$\sqrt{s}$ (TeV)	σ_{LO} (pb)	σ_{NLO} (pb)	σ_{NNLO} (pb)
7	$4.167^{+0.7\%}_{-1.6\%}$	$6.044^{+2.8\%}_{-2.2\%}$	$6.735^{+2.9\%}_{-2.3\%}$
8	$5.060^{+1.6\%}_{-2.7\%}$	$7.369^{+2.8\%}_{-2.3\%}$	$8.284^{+3.0\%}_{-2.3\%}$
9	$5.981^{+2.4\%}_{-3.5\%}$	$8.735^{+2.9\%}_{-2.3\%}$	$9.931^{+3.1\%}_{-2.4\%}$
10	$6.927^{+3.1\%}_{-4.3\%}$	$10.14^{+2.9\%}_{-2.3\%}$	$11.60^{+3.2\%}_{-2.4\%}$
11	$7.895^{+3.8\%}_{-5.0\%}$	$11.57^{+3.0\%}_{-2.4\%}$	$13.34^{+3.2\%}_{-2.4\%}$
12	$8.882^{+4.3\%}_{-5.6\%}$	$13.03^{+3.0\%}_{-2.4\%}$	$15.10^{+3.2\%}_{-2.4\%}$
13	$9.887^{+4.9\%}_{-6.1\%}$	$14.51^{+3.0\%}_{-2.4\%}$	$16.91^{+3.2\%}_{-2.4\%}$
14	$10.91^{+5.4\%}_{-6.7\%}$	$16.01^{+3.0\%}_{-2.4\%}$	$18.77^{+3.2\%}_{-2.4\%}$

TAB. 1.2 –
LO, NLO and NNLO cross sections for on-shell W^+W^- production in the 4FNS and reference results for $gg \to H \to WW^*$ from Ref. [12].

$\sqrt{s}$ (TeV)	σ_{LO} (pb)	σ_{NLO} (pb)	σ_{NNLO} (pb)	$\sigma_{gg\to H\to WW^*}$ (pb)
7	$29.52^{+1.6\%}_{-2.5\%}$	$45.16^{+3.7\%}_{-2.9\%}$	$49.04^{+2.1\%}_{-1.8\%}$	$3.25^{+7.1\%}_{-7.8\%}$
8	$35.50^{+2.4\%}_{-3.5\%}$	$54.77^{+3.7\%}_{-2.9\%}$	$59.84^{+2.2\%}_{-1.9\%}$	$4.14^{+7.2\%}_{-7.8\%}$
13	$67.16^{+5.5\%}_{-6.7\%}$	$106.0^{+4.1\%}_{-3.2\%}$	$118.7^{+2.5\%}_{-2.2\%}$	$9.44^{+7.4\%}_{-7.9\%}$
14	$73.74^{+5.9\%}_{-7.2\%}$	$116.7^{+4.1\%}_{-3.3\%}$	$131.3^{+2.6\%}_{-2.2\%}$	$10.64^{+7.5\%}_{-8.0\%}$

(μ_F) scales are set to $\mu_R = \mu_F = m_W$, and, as done for ZZ production, to assess scale uncertainties they are varied in the range $0.5\,m_W < \mu_{R,F} < 2\,m_W$ with $0.5 < \mu_F/\mu_R < 2$. In the 4FNS we use the pole mass $m_b = 4.75$ GeV. Our NLO and NNLO predictions involve resonant top quarks and off-shell Higgs bosons where we use $m_t = 173.2$ GeV, $\Gamma_t = 1.443$ GeV, $m_H = 125$ GeV and $\Gamma_H = 4.09$ MeV. Higgs contributions, included via squared one-loop amplitudes in the $gg \to H^* \to W^+W^-$ channel, are strongly suppressed since the Higgs boson is off-shell.

In Table 1.2 we present LO, NLO and NNLO predictions for inclusive W^+W^- production in the 4FNS. We see that at 7 (14) TeV the LO predictions receive a positive NLO shift of 53 (58)%, and the NNLO corrections induce a further enhancement by 9 (12)%. This decent perturbative convergence must be relativized, since the scale uncertainty does not decrease significantly when moving from LO to NLO and NNLO. Still, the NNLO corrections exceed the scale uncertainty by about a factor 3.

The fact that the NLO scale variations underestimate higher-order effects can be attributed to the fact that the gluon–gluon partonic channel appears only beyond NLO. The NNLO is the first order at which all partonic channels are contributing. The NNLO scale dependence, which amounts to about 3%, can thus be considered a realistic estimate of the theoretical uncertainty due to missing higher-order effects.

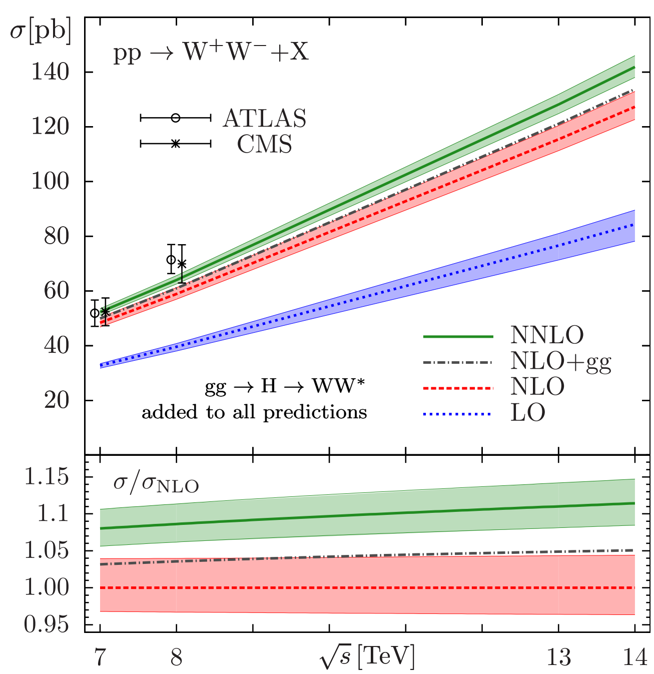

Fig. 1.2 –
Top: the on-shell W^+W^- cross section in the 4FNS at LO, NLO, NLO+gg and NNLO combined with $gg \to H \to WW^*$ is compared with recent ATLAS and CMS results. Bottom: NNLO and NLO+gg results, normalized to NLO. The bands indicate scale variations.

In Fig. 1.2, theoretical predictions in the 4FNS are compared to CMS and ATLAS measurements at 7 and 8 TeV. For a consistent comparison, our results for on-shell W^+W^- production are combined with the $gg \to H \to WW^*$ cross sections reported in Table 1.2. It turns out that the inclusion of the NNLO corrections leads to an excellent description of the data at 7 TeV and decreases the significance of the observed excess at 8 TeV. In the lower frame of Fig. 1.2, predictions and scale variations at NNLO are compared to NLO ones, and also the individual contribution of the $gg \to W^+W^-$ channel is shown. Using NNLO PDFs throughout, the loop induced gluon fusion contribution is only about 35% of the total NNLO correction.

In the light of the small scale dependence of the 4FNS NNLO cross section, the ambiguities associated with the definition of a top-free W^+W^- cross section might represent a significant source of theoretical uncertainty at NNLO. In Ref. [13] we show that the W^+W^- cross-section can be computed within the 5FNS, through an appropriate subtraction of the top contamination based on the scaling behavior of the (N)NLO cross section in the limit of vanishing top-quark width. The obtained results agree within 2% with those obtained in the 4FNS.

The calculation of the second-order QCD corrections described here was accomplished during the past year in a collaborative effort involving many of the researchers at our institute. The timely completion of this project (well ahead of competing groups) is due to unique synergies in our institute, which pools together high-level competences on many different aspects of precision calculations.

[1] J. Wang [ATLAS, D0, CDF and CMS Collaborations], Int. J. Mod. Phys. Conf. Ser. **31** (2014) 1460279.

[2] T. Gehrmann, L. Tancredi and E. Weihs, JHEP **1308** (2013) 070.

[3] J. M. Henn, K. Melnikov and V. A. Smirnov, JHEP **1405** (2014) 090.

[4] T. Gehrmann, A. von Manteuffel, L. Tancredi and E. Weihs, JHEP **1406** (2014) 032.

[5] F. Caola, J. M. Henn, K. Melnikov and V. A. Smirnov, JHEP **1409** (2014) 043.

[6] T. Gehrmann, A. von Manteuffel and L. Tancredi, arXiv:1503.04812 [hep-ph].

[7] S. Catani and M. Grazzini, Phys. Rev. Lett. **98** (2007) 222002.

[8] F. Cascioli, T. Gehrmann, M. Grazzini, S. Kallweit, P. Maierhöfer, A. von Manteuffel, S. Pozzorini and D. Rathlev *et al.*, Phys. Lett. B **735** (2014) 311.

[9] T. Gehrmann, M. Grazzini, S. Kallweit, P. Maierhöfer, A. von Manteuffel, S. Pozzorini, D. Rathlev and L. Tancredi, Phys. Rev. Lett. **113** (2014) 21, 212001.

[10] F. Cascioli, P. Maierhöfer and S. Pozzorini, Phys. Rev. Lett. **108** (2012) 111601.

[11] A. D. Martin, W. J. Stirling, R. S. Thorne and G. Watt, Eur. Phys. J. C **63** (2009) 189.

[12] S. Heinemeyer *et al.* [LHC Higgs Cross Section Working Group Collaboration], arXiv:1307.1347 [hep-ph].

[13] T. Gehrmann, M. Grazzini, S. Kallweit, P. Maierhöfer, A. von Manteuffel, S. Pozzorini, D. Rathlev and L. Tancredi, Phys. Rev. Lett. **113** (2014) 21, 212001.

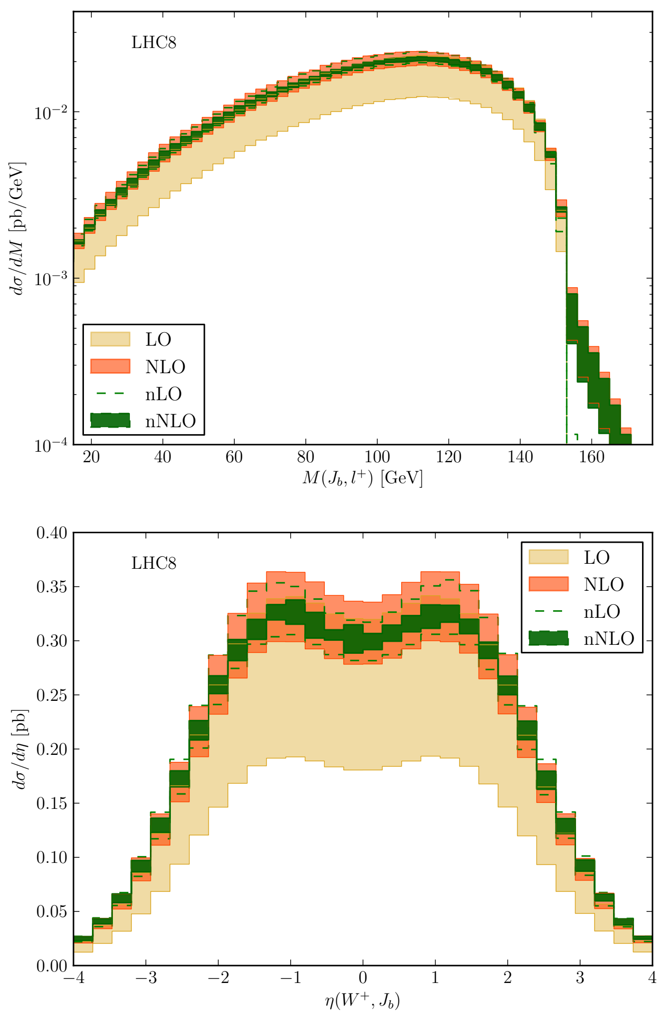

FIG. 1.3 – Invariant mass of the b-jet lepton pair (top panel) and pseudo-rapidity of the reconstructed top (bottom panel) for the 8 TeV LHC with standard cuts as described in the text. The approximate NNLO prediction is denoted by nNLO

1.2 Differential cross sections for top pair production beyond NLO

At the LHC, top quarks are produced predominantly as $(t\bar{t})$ pairs. A precise theoretical understanding of this process is important both for the determination of the top quark mass and for numerous studies in which the process forms a background. Since top quarks decay almost instantly through $t \to W^+ b$ and $\bar{t} \to W^- \bar{b}$, with subsequent W decay, they are detected indirectly through their decay products. Hence, for a realistic description it is essential to include the top decay and allow for cuts mimicking the experimental selection procedures.

In Ref. [1] results for fully differential top-pair production have been presented that go beyond a full NLO calculation: approximate NNLO correction terms (denoted by nNLO) in the production of a $t\bar{t}$-pair have been included. Renormalization-group techniques were applied to determine NNLO terms that are enhanced by logarithms. Near threshold, these terms are expected to dominate and thus give a reliable estimate of the full correction. The precise form of these logarithmic corrections depends on the kinematic situation and several options have been investigated, giving consistent results.

As an example, in Fig. 1.3 two distributions are shown for the 8 TeV LHC. The k_T-cluster algorithm has been applied to define b-jets J_b and as an illustration the following standard cuts on the decay products J_b, l and ν have been applied: $p_T(J_b) > 15$ GeV, $E_T(l) > 15$ GeV and $\not{E}_T > 20$ GeV. The comparison of the full NLO result with the approximate NLO result strongly indicates that the nNLO results are a reliable improvement beyond NLO.

[1] A. Broggio, A. S. Papanastasiou and A. Signer, JHEP **1410** (2014) 98.

1.3 Pseudo observables in Higgs decays

After the discovery phase, Higgs physics has entered the era of precision measurements. Characterizing the particle properties accurately and with minimal theoretical bias, is of utmost importance when investigating the nature of physics beyond the Standard Model. For this reason we have developed a formalism characterizing Higgs decays in generic extensions of the SM with heavy new particles. Ref. [1]. The method uses a set of *pseudo observables* (PO) defined by the momentum expansion of the on-shell Higgs decay amplitudes. More precisely, the PO of a generic Higgs to n-body decay are defined by the expansion of the decay amplitude around the single-particle poles (in all $m < n$ relevant subsystems) due to the exchange of SM particles.

The PO are well-defined physical parameters that can be directly extracted from data, providing a natural generalization of the so-called "κ-framework" introduced so far by the LHC collaborations. Moreover, they allow for a systematic inclusion of higher-order QED and QCD corrections and can be computed in any Effective Field Theory (EFT) approach to Higgs physics. The number of independent PO reduces when applying certain hypotheses such as lepton-universality, CP invariance, custodial symmetry, and linearly realized electroweak symmetry breaking.

[1] M. Gonzalez-Alonso, A. Greljo, G. Isidori and D. Marzocca, Eur. Phys. J. C **75** (2015) 3, 128.

1.4 Extending the Standard Model up to Infinite Energy

Attempts to solve naturalness by having the weak scale as the only breaking of classical scale invariance have to deal with two severe difficulties: gravity and the absence of Landau poles. We have shown that solutions to the first problem require premature modifications of gravity at scales no larger than 10^{11} GeV, while the second problem calls for many new particles around the weak scale Ref. [1].

In order to build models that fulfill these properties, we have classified the four-dimensional Quantum Field Theories that satisfy the criterion of Total Asymptotic Freedom (TAF), namely theories that hold at any energy scale, with all coupling constants flowing to zero. We have developed a method identifying such theories and determining their low-energy predictions. Since the Standard Model turns out to be asymptotically free only under unphysical conditions, we have explored some of its weak-scale extensions that satisfy the requirements for TAF. Interestingly, the latter predict a large number of new particles around the TeV scale which are, however, severely constrained by low-energy flavor data. In that perspective, a significant amount of fine-tuning is required.

[1] G. F. Giudice, G. Isidori, A. Salvio and A. Strumia, JHEP **1502** (2015) 137.